JOURNAL OF MATERIALS SCIENCE **35** (2000) 6259–6266

Influence of repetitive stiffness variation on crack growth behaviour in wood

F. THUVANDER
Division of Polymer Engineering, Luleå University of Technology, SE-97187 Luleå, Sweden
L. O. JERNKVIST, J. GUNNARS
Division of Solid Mechanics, Luleå University of Technology, SE-97187 Luleå, Sweden
E-mail: loje@mt.luth.se

Softwoods have a repetitive variation in stiffness over their growth rings, which is due to the difference in cellular structure between the latewood and earlywood. In this paper, the influence of the repetitive stiffness variation on radially growing cracks is studied by detailed finite element analyses, in which the wood material is represented by a layered orthotropic continuum. The distribution of stress around the crack is found to be very different from crack tip stress fields in homogenous isotropic materials. The latewood layer ahead of the crack experiences a significant tensile stress, which indicates that formation of new secondary cracks ahead of the primary crack front is a likely mechanism for crack propagation. This mechanism is also favoured by the fact that the primary crack is subjected to a significant shielding from the stiff latewood, which tends to arrest the primary crack in the soft earlywood layer. Analyses are performed for materials with various growth ring widths, and the calculated results are compared with reported experimental observations.

1. Introduction

Wood has been used as a material for construction, tools, furniture and decoration for thousands of years. However, many details of its fracture behaviour is not yet understood. Knowledge of the fracture behaviour has relevance not only to the structural use of wood, but has also importance to processes like cutting and machining.

Wood consists of tubular stiff cells, in softwood called tracheids, which are connected by a weaker material called the middle lamella. The cell walls have a layered structure, where each layer has distinctive material properties that together determine the properties of the walls. Softwoods growing in a temperate climate form growth rings, see Fig. 1. A low density material with large cells is formed early in the season of growth, whereas a dense material with thicker cell walls is formed later in the season. The annual alteration between these two materials, termed earlywood and latewood, produces a repetitive density variation in the radial direction of the stem. The variation of the cellular structure within the growth rings also induces a repetitive gradient for the stiffness. It may be noted that, at a macroscopic level, the density is strongly correlated to wood material properties, such as stiffness and strength [1, 2].

Wood is a highly anisotropic material with the principal axes of anisotropy conventionally denoted, *R*, *T* and *L* for the radial, tangential and longitudinal direction, respectively. The elastic modulus in the longitudinal direction is about one order of magnitude higher than in the other two directions. Also the fracture behaviour is linked to the material structure and six principal systems of crack propagation can be identified by material symmetry, [3]. Each system is commonly identified with a pair of letters, the first indicating the crack surface normal and the second describing the direction of crack growth. The concept of fracture mechanics has been applied to quantify and describe fracture of wood at a macroscopic level within these fracture systems. The influence of density, moisture and drying process etc. on the fracture toughness has been experimentally studied [2, 4–7]. In general, fracture toughness in the *LT* and *LR* systems is about an order of magnitude higher than in the other systems. The *LT* and *LR* systems correspond to crack growth across the tracheids, which takes place mainly by cell wall tearing. The other systems are associated with crack growth along the tracheids, usually through a peeling fracture mode. This tracheid separation, in or close to the middle lamella, leaves the cell walls intact and the lumens are not exposed [8, 9].

A significant difference in fracture toughness is also found when the *TL* and *TR* systems are compared, although the crack surface normals are identical and the local fracture mechanism at the crack front, tracheid separation, is the same for these two systems. The

F. Thuvander is currently at: Department of Materials Science, Karlstad University, SE-651 88 Karlstad, Sweden
J. Gunnars is currently at: DNVAS, P.O. Box 49306, SE-100 29 Stockholm, Sweden

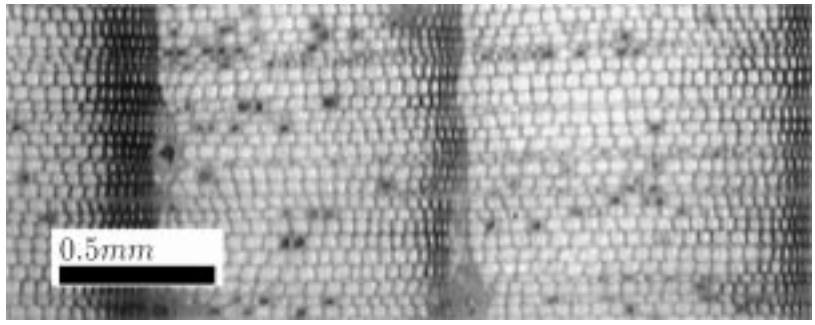

Figure 1 Typical growth ring structure for pine, *Pinus Sylvestris L.*, from the northern coastal region of Sweden.

measured fracture toughness in Douglas fir is typically 30–50% higher in the *TR* system than in the *TL* system [10–12], and even larger differences have been reported for pine and spruce [13, 14]. We suggest that the difference in fracture toughness between the *TR* and *TL* systems could be explained by the repetitive stiffness gradient, induced by the growth rings. The gradient will affect a *TR* crack, which is propagating across the growth rings, whereas a crack propagating in the *TL* system is largely unaffected.

Linear elastic fracture mechanics predicts that a crack growing towards a sharp interface to a stiffer material experiences a reduced stress intensity, as compared with the homogenous case, when the interface is approached [15]. The reduced near tip stress intensity results in an increased macroscopic fracture toughness of the material. Inversely, as a crack approaches an interface to a more compliant material, the stress concentration near the crack tip is intensified. These shielding and amplification effects are similar for a crack growing in a material with a continous change of the elastic properties [16], but the effects are weaker.

A *TR* crack grows across the growth rings and experiences a repetitive variation in the elastic properties. As the crack approaches the stiffer latewood material at some position, crack tip shielding offers a possible mechanism for crack arrest both for growth towards the pith and towards the bark. The shielding is strongest for the crack growing towards a sharp stiffness interface, i.e. for the crack growing towards the pith. Experimental results from measurements of fracture toughness in a *TR* system as function of crack tip position within a single growth ring strongly demonstrate these effects [17].

In this paper, the effect of a repetitive stiffness gradient on a crack growing across the growth rings is studied by finite element analysis. The studied configuration corresponds to a crack propagating in the *TR* system from bark to pith. The material properties, including the repetitive stiffness variation, are chosen to be representative of *Pinus sylvestris L*. The influence of the stiffness variation on crack growth behaviour is evaluated by studying the near tip $J-$integral and the stress and strain state ahead of the crack.

2. Model description

A two-dimensional finite element model is used to simulate crack propagation in a small CT-specimen. The crack is assumed to grow radially from bark to pith, crossing the growth rings perpendicularly, or with a small inclination to the radial direction.

2.1. Material properties

At a sufficient distance from the pith, the curvature of the growth rings can be neglected and the wood material locally considered as rectilinearly orthotropic. In our analysis, the material is represented by an inhomogenous continuum with a linear elastic orthotropic stress-strain relation. In a plane perpendicular to the tracheids, this relation can be written

$$\begin{pmatrix} \varepsilon_R \\ \varepsilon_T \\ \varepsilon_L \\ \varepsilon_{RT} \end{pmatrix} = \begin{bmatrix} \frac{1}{E_R} & \frac{-\nu_{RT}}{E_T} & \frac{-\nu_{RL}}{E_L} & 0 \\ \frac{-\nu_{TR}}{E_R} & \frac{1}{E_T} & \frac{-\nu_{TL}}{E_L} & 0 \\ \frac{-\nu_{LR}}{E_R} & \frac{-\nu_{LT}}{E_T} & \frac{1}{E_L} & 0 \\ 0 & 0 & 0 & \frac{1}{2G_{RT}} \end{bmatrix} \begin{pmatrix} \sigma_R \\ \sigma_T \\ \sigma_L \\ \sigma_{RT} \end{pmatrix} \quad (1)$$

where ε_i and σ_i are the strain and stress components, and E_i, G_{ij} and ν_{ij} are the elastic constants.

The elastic constants in Equation 1 represent a continuum model for the cellular wood structure. The constants are dependent on both the wood cell geometry and the cell wall elastic properties. Gibson and Ashby [1] have proposed a simple model, from which the in-plane elastic constants can be determined by representing the wood microstructure as a two-dimensional regular honeycomb, see Fig. 2.

By considering the hexagonal unit cell in Fig. 2 as a framework structure, equivalent stiffness parameters

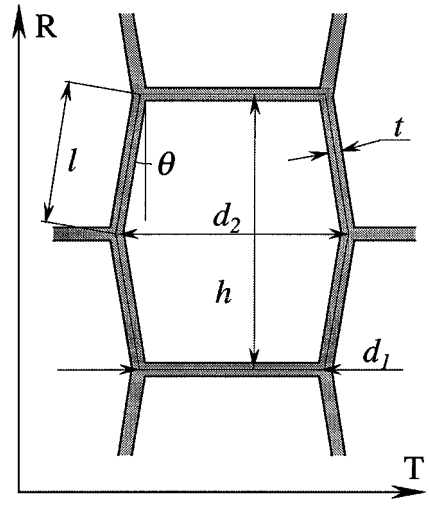

Figure 2 The hexagonal unit cell approximation of the tracheids.

can be derived from simple beam theory. The expressions are [1]

$$E_R^b = \frac{E_t \cos\theta}{(d_1/l + \sin\theta)\sin^2\theta}\left(\frac{t}{l}\right)^3 \quad (2)$$

$$E_T^b = \frac{E_t(d_1/l + \sin\theta)}{\cos^3\theta}\left(\frac{t}{l}\right)^3 \quad (3)$$

$$G_{RT} = \frac{E_t(d_1/l + \sin\theta)}{(1 + 2d_1/l)\cos\theta}\left(\frac{l}{d_1}\right)^2\left(\frac{t}{l}\right)^3 \quad (4)$$

$$\nu_{RT} = \frac{(d_1/l + \sin\theta)}{\cos\theta}\tan\theta \quad (5)$$

where the parameters t, l, d_1 and θ are defined in Fig. 2, and E_t denotes the transverse stiffness of the cell wall. The effective longitudinal stiffness of the unit cell is given by

$$E_L = E_l \frac{\rho}{\rho_0} \quad (6)$$

where E_l is the longitudinal cell wall stiffness and ρ/ρ_0 is the fraction of cell average density to the cell wall density. It is calculated from the fractional area of cell walls in the unit cell cross section

$$\frac{\rho}{\rho_0} = \frac{(2 + d_1/l)}{2(d_1/l + \sin\theta)\cos\theta}\left(\frac{t}{l}\right) \quad (7)$$

The moduli given by Equations 2 and 3 are derived by identifying bending as the only mode of cell wall deformation. This assumption leads to an overestimated stiffness, especially when the cell wall thickness is large. The model is further improved by considering compression of the cell walls as an additional deformation mechanism, and the final expressions for E_R and E_T are thereby found from

$$E_R = \frac{E_R^b E_R^c}{E_R^b + E_R^c} \quad (8)$$

$$E_T = \frac{E_T^b E_T^c}{E_T^b + E_T^c} \quad (9)$$

where the effective stiffnesses from compression are

$$E_R^c = E_t \frac{t}{d_1} \quad (10)$$

$$E_T^c = E_t \frac{t}{2l\cos\theta} \quad (11)$$

Values for the cell wall double moduli E_t and E_l have been taken from the literature [1], and are assumed to be the same in latewood and earlywood, see Table I. This is an approximation, since the fraction of the secondary cell wall layer, S2, increases from earlywood to latewood, thereby introducing a difference in cell wall elastic properties across the growth ring.

The geometry of the tracheids varies significantly from earlywood to latewood. This variation was quantified by examination of micrographs. Based on the examination, the growth rings were divided into three

TABLE I Cell wall properties and cell geometry

Cell wall property		Cell geometry		
			Earlywood	*Latewood*
E_l	40 GPa	t	3.2 μm	5.7 μm
E_t	10 GPa	h	34 μm	17 μm
ρ_0	1500 kgm^{-3}	d_1	25 μm	25 μm
		d_2	27 μm	27 μm

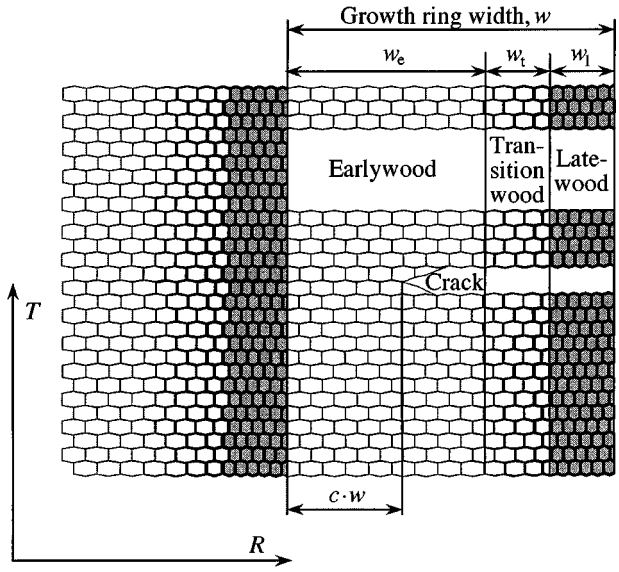

Figure 3 The three radial zones of the growth ring.

radial zones with different cell geometry; earlywood, latewood and transitionwood, as shown in Fig. 3. Moreover, it was found that a constant thickness of the latewood, w_l, of 200 μm could be assumed, whereas the thickness of the transitionwood, w_t, was found to occupy 20% of the entire growth ring width, w. A similar model was used by Persson [18] to determine the elastic properties for spruce.

The cell wall double thickness, t, and the cell height, h, were set to be constant in the earlywood and latewood, whereas an exponential variation was assumed in the interjacent transitionwood. The tangential width of the cells was found to be fairly constant in all three regions of the growth ring, and a constant cell width was therefore used. The width at the cell-to-cell interfaces, d_1 and at the midcell bulge, d_2, are defined in Fig. 2. The values used for these quantities are given in Table I. The out-of-plane Poisson ratios, ν_{RL} and ν_{TL}, were given the constant value of 0.45 [1].

2.2. Finite element model

The two-dimensional plane strain finite element model of the CT-specimen geometry is shown in Fig. 4. An inward growing crack, having an inclination α with respect to the radial direction, was examined. The specimen was subjected to a tensile opening load, applied through a pair of point loads, indicated in Fig. 4. A constant load, F, of 10 N was used throughout the investigation.

Close to the crack tip, a region corresponding to five growth rings was modelled with a repetitive stiffness

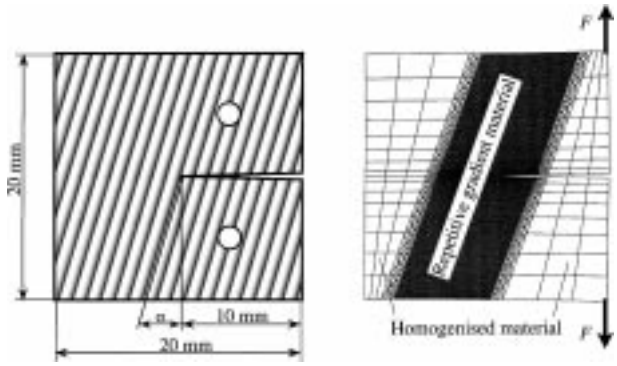

Figure 4 Finite element mesh and specimen dimensions.

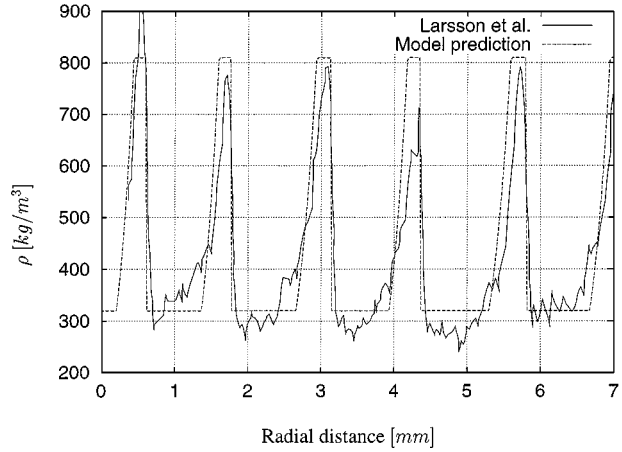

Figure 5 Density variation across growth rings.

gradient. The material outside this region was given homogeneous properties, see section 3.1. The stiffness gradient in the five growth rings was deduced from Equations 2–11, with the assumed tracheid cell properties given in Table I. A rectilinear orthotropic elastic material model was used. Within each of the five growth rings, the radial variation in stiffness was resolved by use of 25 layers of elements, where each layer was given individual stiffness properties, corresponding to its position within the growth ring.

A total number of 16768 linear elements were used in the finite element model. The mesh was locally refined close to the crack tip, thereby facilitating calculation of the near-tip J-integral along a contour that was fully encompassed by a single layer of homogenous material. The indefiniteness, which inevitably arises when evaluating J in a material with a stiffness gradient in the crack propagation direction, was thus avoided [19]. The finite element model was parametrisised with respect to the crack inclination angle, α, the growth ring width, w, and the crack tip position within the growth ring, c, see Figs 3 and 4.

3. Results and discussion

3.1. Verification of the material model

An attempt was first made to verify the assumed repetitive stiffness gradient with experimental data. Since detailed information on the actual stiffness variation across the growth rings in *Pinus silvestris L.* is not available, measured average stiffnesses found in the literature were used to evaluate the material model.

The average elastic constants for a unit cell consisting of five growth rings with the repetitive stiffness gradient given by Equations 2–11 were determined by finite element calculations. The unit cell was subjected to homogeneous boundary conditions, corresponding to uniaxial tension and simple shear, and the homogenised values E_i^h, $i = R, T, L$, G_{RT}^h, ν_{RT}^h and ν_{TR}^h were determined. For a growth ring width, w, of 1.6 mm, the calculated homogenised elastic moduli E_R^h and E_T^h were 1.38 and 0.57 GPa respectively. These results are in reasonable agreement with the experimentally determined moduli of 1.10 and 0.57 GPa reported in [20]. The effective value of E_R^h is somewhat overestimated, which is probably an effect of the perfect radial alignment of tracheids assumed in our model. The perfectly aligned configuration yields a higher radial stiffness than the actual wood structure, which exhibits a slight irregular zig-zag pattern in the radial direction. The influence of these irregularities on the elastic properties has been investigated by Kahle and Woodhouse for Norway spruce [21]. They reported that E_R is significantly reduced by the cell wall kinking.

The density variation was calculated with Equation 7 from our approximate geometrical variation and is shown in Fig. 5. The calculated density is compared with X-ray microdensiometry measurements from Larsson *et al.* [22].

3.2. Calculated stress and strain distributions

A typical distribution for the tangential stress, σ_T, in the vicinity of the crack tip is presented in Fig. 6. The

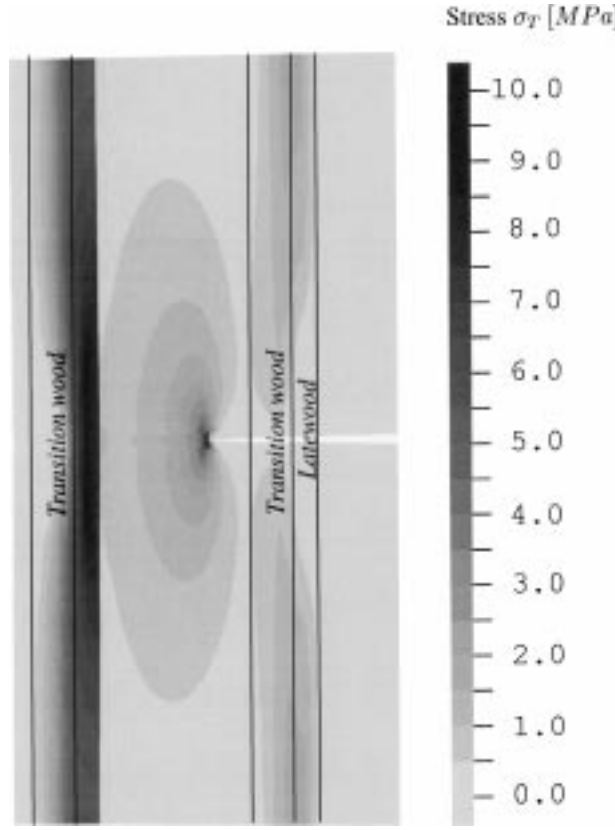

Figure 6 Distribution of tangential stress, σ_T, for a growth ring width, ω, of 1.6 mm.

crack extends from the bark to the pith along the radial direction, $\alpha = 0$. The analysis was made for a growth ring width of 1.6 mm, with the crack tip positioned in the growth ring centre, $c = 0.5$. The tangential stiffness for the latewood is about 20 times as high as for the earlywood, wheareas the stiffness ratio in the radial direction is about 2.

Fig. 6 reveals high stresses in the stiff latewood layer ahead of the crack tip, and the latewood layer carries a substantial part of the total tensile load. Furthermore, the highly stressed region in the latewood has a tangential width, which is considerably larger than the width of the growth ring. A singular stress field prevails at the crack tip, but the area dominated by the singular field is confined to the earlywood region of a single growth ring. The stress field calculated by this homogenised material model is, due to the cellular microstructure, of course not expected to represent the detailed state at distances from the crack tip comparable to the tracheid width.

The tangential strain is shown in Fig. 7. As evident from the figure, the crack tip strain field is trapped between the latewood layer ahead and astern of the tip. The stiff latewood layers ahead and astern distribute the imposed load over the earlywood. This causes the strain field to spread in the tangential direction within the compliant earlywood layer. Measurements of the strain field at the crack tip presented by Thuvander *et al.* [23] are in agreement with the calculated strains.

We conclude that the distribution of stress and strain around the crack is strongly affected by the growth rings. Thus, the stiffness gradient must be accounted for in crack growth analyses. In particular, the stress distribution in the latewood layer ahead of the crack needs to be considered.

3.3. Influence of crack tip position

The stress distribution in the latewood layer ahead of the crack is affected by the crack tip position within the growth ring. In Fig. 8, the calculated average tangential stress, σ_T, in the latewood layer ahead of the crack tip is shown for a growth ring width, w, of 1.6 mm. The results are given for seven different relative crack tip positions, c. The tangential stress is plotted with respect to the $z-$coordinate, which is the distance from the crack plane, see insert in Fig. 8. The tangential stress increases monotonously as the crack approaches the latewood layer. Irrespective of the crack tip position, a peak stress region in the latewood layer can be discerned, the tangential width of which is approximately twice the growth ring width. The stresses are high also outside this peak region .

The calculated J-integral as a function of relative crack tip position within the 1.6 mm wide growth ring is presented in Fig. 9. As the crack passes through the latewood layer and proceeds into the transitionwood, J increases rapidly and reaches a maximum value before the

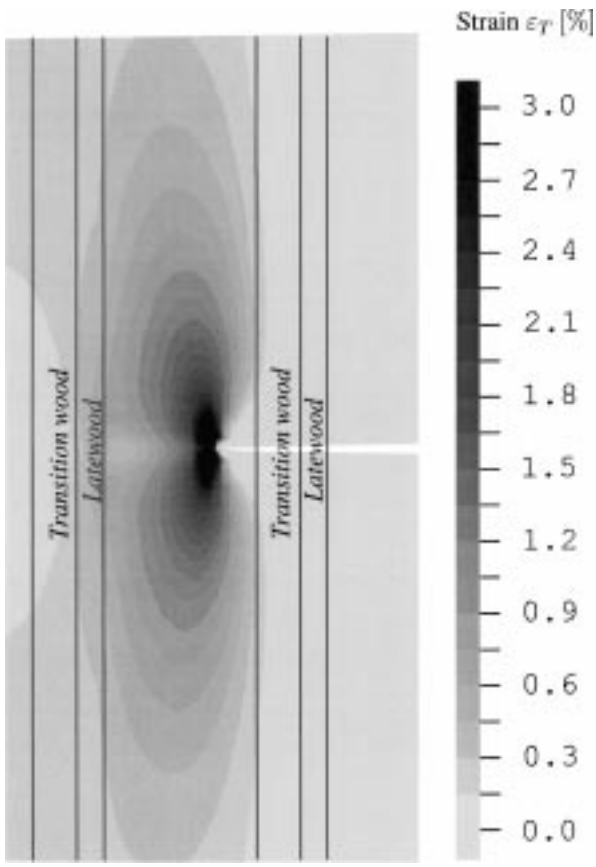

Figure 7 Distribution of tangential strain, ε_T, for a growth ring width, w, of 1.6 mm.

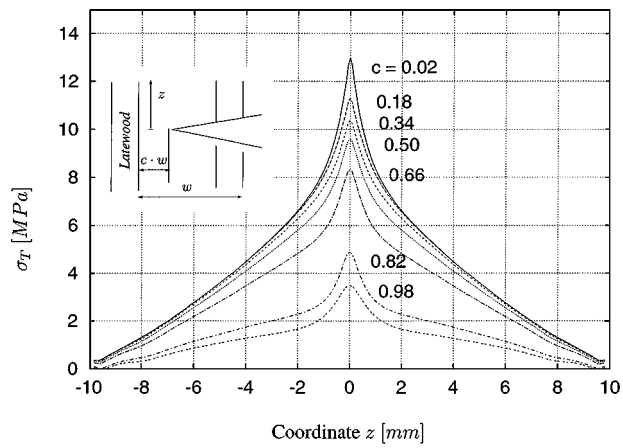

Figure 8 Distribution of tangential stress in the latewood layer ahead of the crack for different relative crack tip positions, c. Growth ring width, w, 1.6 mm.

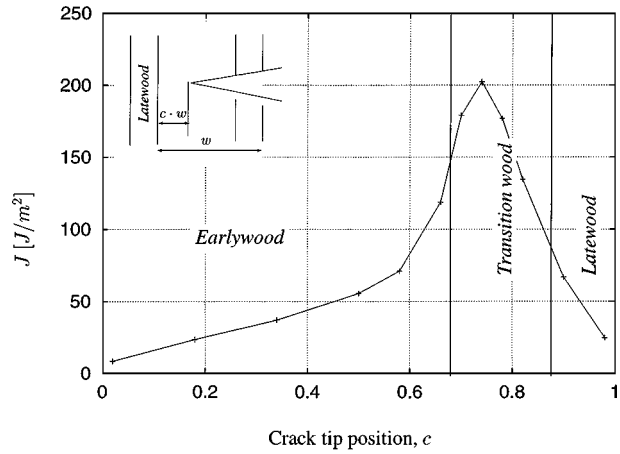

Figure 9 J-integral for different positions of the crack. Growth ring width, w, 1.6 mm.

crack tip enters the earlywood, at $c \approx 0.7$. Further crack propagation into the earlywood results in a decreasing value for J as the latewood layer is approached. This decline of J with increasing crack length under constant imposed load gives a possible mechanism for crack arrest, provided that the fracture toughness is independent of the crack tip position, c. Since the earlywood structure is fairly homogeneous, there is no indication of a significant variation of the fracture toughness. This implies that the gradient in stiffness, caused by the growth rings, induces a mechanism for crack arrest. Furthermore, the crack will be arrested at a position $c < 0.7$ were J is decreasing, which corresponds to a position in the earlywood layer. This is supported by experimental observations of cracks arrested in the earlywood layer [10, 24]. The variation of J within the growth ring is also in agreement with experiments performed by Ando and Ohta [17]. They measured the fracture toughness variation within a growth ring for air dried specimens of *Picea sitchensis*, and found that the fracture toughness for a crack growing from the bark side increases as the crack tip is positioned closer to the latewood layer ahead. An increase in fracture toughness corresponds to a decline in near-tip driving force for fracture, J. Ashby *et al.* [8] observed *TR* cracks propagating in ash. In this material, cracks were found to arrest at clusters of sap channels, which correspond to compliant regions.

Once arrested, the crack may resume propagation either if the external load is raised, or if the load is redistributed within the material in such a way that the stress intensity at the crack tip increases. In view of the stress concentration found in the latewood layer ahead of the crack, such a redistribution could be effectuated through creep relaxation of the highly stressed latewood material. This would result in an apparent decline in fracture toughness for long term loading.

Another possible mechanism for further crack growth in the *TR* system is given by formation of secondary cracks at defects located in the highly stressed latewood layer ahead of the primary crack. Defects in the form of intertracheid flaws, ray cells and resin channels are abundant in most softwoods, particulary after a seasoning process, and these defects may serve as nucleation sites for cracks. A secondary crack will first break the stiff latewood layer, after which the bridging ligament between the primary and secondary crack is broken and a single connected crack is formed. This mechanism was observed in references [10, 24].

Considering the high tangential stress, which is distributed over a large region in the latewood layer ahead of the crack, it is likely that secondary cracks may form at flaws located away from the primary crack plane. This implies that the crack plane has a tendency to jump in the tangential direction, which is in accordance with fractographic examinations of *TR* cracks [25]. This is also visible in the pictures of crack paths presented by Ashby *et al.* [8] and Schniewind and Pozniak [10]. Furthermore, the latewood layer stress distribution depicted in Fig. 8 suggests that these jumps could be comparable in size to the growth ring width. The magnitude of the jump is also dependent on the density and size distribution of defects in the latewood layer. A high frequency of evenly distributed small defects would imply small deviations of the crack plane.

3.4. Influence of crack inclination

So far, we have studied a crack propagating in pure *TR*-mode, i.e. along the radial direction. Next, we will examine crack propagation in other directions by varying the angle of incidence with respect to the stiffness gradient, α. Since the middle lamellas constitute radially oriented surfaces with low toughness, the tangential stress in the latewood layer is crucial for fracture initiation. Consequently, the tangential stress is studied and not the maximum principal stress. In addition, these stresses almost coincide for moderate α. Fig. 10 shows the average tangential stress in the latewood layer ahead of the tip for $\alpha = 20^\circ$. The stress is calculated for various positions of the crack tip within a 1.6 mm wide growth ring. The peak stress position is somewhat displaced, but a comparison with Fig. 8 shows that the stress distribution is only weakly affected for this moderate variation in crack inclination.

The J-integral as a function of crack tip position is given for three different values of inclination angles, α, in Fig. 11. Evidently, the angle of inclination has only a minor influence on J in this range. Since neither

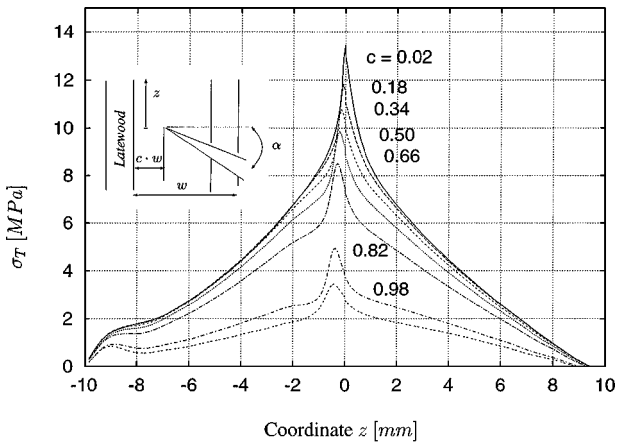

Figure 10 Average tangential stress, σ_T, in the latewood layer ahead of the crack. Inclination angle, $\alpha = 20^\circ$. Growth ring width, w, 1.6 mm.

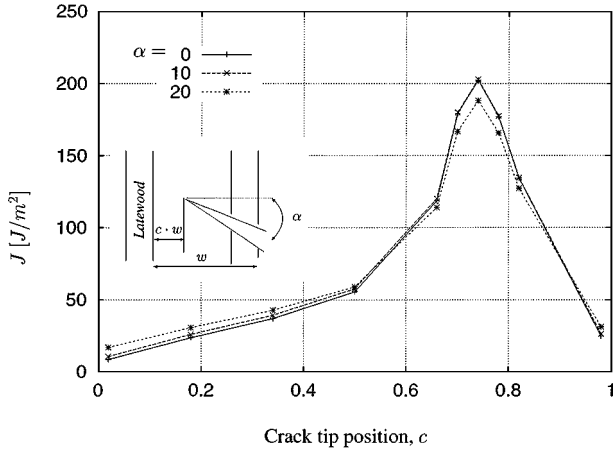

Figure 11 J-integral for different crack inclinations, α. ($w = 1.6$ mm).

J, nor the stress distribution is notably affected by the crack inclination, the remarks made in section 3.3 about crack arrest and formation of secondary cracks in the latewood layer ahead of the tip apply also for oblique cracks.

Thuvander and Berglund [24] observed that the formation of a secondary crack in the latewood layer ahead of an oblique crack causes a change in direction towards pure *TR*-mode for the continued crack growth after the latewood layer is passed. The tendency for oblique cracks to deviate into pure *TR* propagation was also observed by Boatright and Garret [26] and Ashby *et al.* [8]. This kind of crack deflection is generally explained by a difference in fracture toughness between the pure radial and oblique crack propagation directions [8, 26]. In view of the material cellular structure, such a difference is likely, since crack growth in the pure radial direction can proceed without kinking by separation at the middle lamella. However, the stress distribution may also contribute to pure radial crack growth. The high tensile tangential stress promotes formation of a secondary crack in the pure radial direction within the latewood layer ahead of the primary crack. Thus, when a secondary crack is initiated ahead of an arrested crack, the growth ring induced stiffness variation will by itself divert the crack towards pure *TR* growth.

Moreover, He and Hutchinson [27] analysed a crack approaching an interface at an oblique angle in isotropic materials. They concluded that a crack approaching a stiffer material will curve away from the interface, and inversely, an oblique crack approaching a more complient material will tend to grow prependicularly towards the interface. Disregarding the anisotropy in elastic and fracture properties present in our case, this implies that an oblique crack has a tendency to curve towards pure radial growth for crack tip positions within the latewood layer, and the inclined crack has a propensity to deflect from radial growth for positions within the earlywood layer.

3.5. Influence of growth ring width

The following discussion on the influence of growth ring width is confined to cracks propagating in the radial inward direction, $\alpha = 0$, i.e. pure *TR* fracture. Fig. 12 shows the average tangential stress in the latewood layer ahead of the crack tip for two different growth ring widths, 1.2 and 2.0 mm, respectively. By comparing these cases with the stress distribution for a growth ring width of 1.6 mm in Fig. 8, we see that the stress level decreases with increasing growth ring width. This is expected, since the absolute distance between the crack tip and the latewood layer ahead increases for wider growth rings. The peak of the tangential stress is lower and blunter for the wider growth ring, which results in an increased sensitivity to defects aside of the crack plane. Hence, larger deviations from the crack plane is expected and therefore rougher crack surfaces will be formed in a material with wide growth rings [25].

The J-integral as a function of the relative crack tip position for different growth ring widths is shown in Fig. 13. The peak value of J increases with growth ring

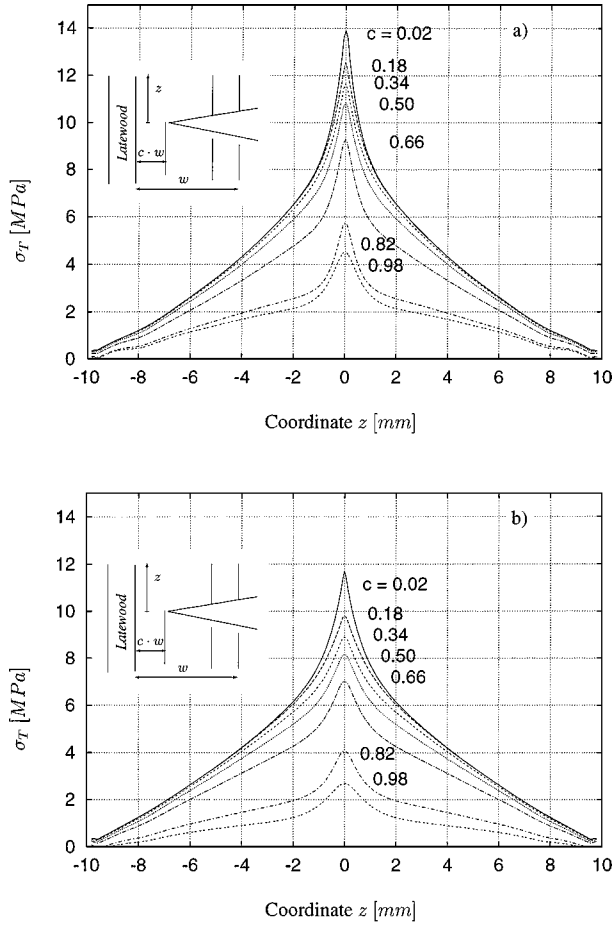

Figure 12 Average tangential stress, σ_T in the latewood layer ahead of the crack for two different widths of the growth ring, (a) $w = 1.2$ and (b) $w = 2.0$ mm.

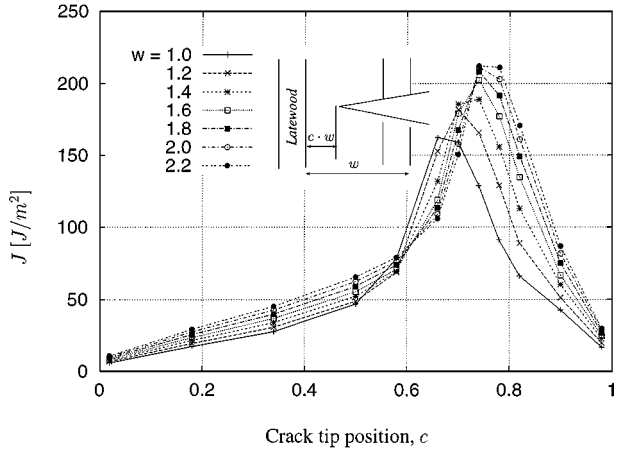

Figure 13 J-integral for different widths, w, of the growth ring.

width, and the peak position is found at the interface between the earlywood and the transitionwood. The amount of latewood is held constant for the different growth ring widths. Thus, the interface moves from $c \approx 0.7$ for a growth ring width of 2.2 mm to $c \approx 0.6$ for a width of 1.0 mm. From Fig. 13, it is also clear that the variation of J over the growth ring decreases for narrow growth rings. Supported by this observation, we may conclude that the mechanism for crack arrest is stronger in a material with wider growth rings.

4. Conclusions

Finite element analyses of a crack extending from bark to pith in the *TR* system of a typical softwood show that the stress state around the crack is strongly affected by the growth ring induced stiffness variation. The repetitive stiffness gradient must therefore be considered in analysis of crack growth mechanisms.

The latewood layer ahead of the tip carries a significant stress over a region, whose tangential extension is considerably larger than the width of the growth rings. It is therefore likely that secondary cracks form at defects in the latewood layer ahead of the crack tip, also when these defects are located away from the primary crack plane. An irregular crack surface will thereby be formed, and the stress analysis indicates that larger deviations of the crack plane are expected for wider growth rings.

The formation of secondary cracks in the latewood layer ahead of the primary crack also provides a mechanism for aligning oblique cracks into pure radial crack growth. Thus, the stiffness variation alone will divert a crack toward pure *TR* growth.

From the calculated variation in the J-integral, it is clear that the stiff latewood layer ahead of the crack effectively shields the crack tip and thus the growth ring induced stiffness gradient provides a mechanism for crack arrest in the earlywood. This is in agreement with reported experimental results, and is also a likely explanation to the difference in fracture toughness between the *TR* and *TL* crack systems. Moreover, the mechanism for crack arrest is more pronounced in materials with wide growth rings.

Acknowledgements

Financial support from the Swedish Council for Forestry and Agricultural Research (SJFR) for F. Thuvander, and from the Swedish Foundation for Strategic Research (SSF) for L.O. Jernkvist, is gratefully acknowledged.

References

1. L. J. GIBSON and M. F. ASHBY, "Cellular Solids: Structure and Properties" (Pergamon Press, Oxford, 1988).
2. A. P. SCHNIEWIND, T. OHGAMA, T. AOKI and T. YAMADA, *Wood Sci.* **15** (1982) 101.
3. J. BODIG and B. A. JAYNE, "Mechanics of Wood and Wood Composites" (Van Nostrand Reinhold, New York, 1982).
4. M. M. GAPPOEV, *Ind. Lab.* **60** (1994) 680.
5. G. PROKOPSKI, *Int. J. Fract.* **79** (1996) R73.
6. S. E. STANZL-TSCHEGG, E. K. TSCHEGG and A. TEISCHINGER, *Wood Fiber Sci.* **26** (1994) 476.
7. B. YEH and A. P. SCHNIEWIND, *ibid.* **24** (1992) 364.
8. M. F. ASHBY, K. E. EASTERLING, R. HARRYSSON and S. K. MAITI, *Proc. R. Soc. London A* **398** (1985) 261.
9. G. R. DEBAISE, A. W. PORTER and R. E. PENTONEY, *Mater. Res. Stand.* **6** (1966) 493.
10. A. P. SCHNIEWIND and R. A. POZNIAK, *Eng. Fract. Mech.* **2** (1971) 223.
11. S. MINDESS, J. S. NADEAU and J. D. BARRET, *Wood Sci.* **8** (1975) 389.
12. A. P. SCHNIEWIND and J. C. CENTENO, *Wood Fiber* **5** (1973) 152.
13. K. RIIPOLA and M. FONSELIUS, *Journal of Structural Engineering* **118** (1992) 1741.
14. M. FONSELIUS and K. RIIPOLA, *ibid.* **118** (1992) 1727.
15. T. S. COOK and F. ERDOGAN, *Int. J. Engng Sci.* **10** (1972) 677.
16. F. ERDOGAN, A. C. KAYA and P. F. JOSEPH, *J. Appl. Mech.* **58** (1991) 410.
17. K. ANDO and M. OHTA, *Mokuzai Gakkaishi* **41** (1995) 640.
18. K. PERSSON, Report TVSM-3020, Lund University, Sweden, 1997.
19. Report ARD 97-7, ADINA R & D Inc, Watertown, MA, 1997.
20. F. F. P. KOLLMANN and W. A. CÔTÉ, "Principles of Wood Science and Technology, I: Solid Wood" (Springer Verlag, New York, 1968).
21. E. KAHLE and J. WOODHOUSE, *J. Mater. Sci.* **29** (1994) 1250.
22. B. LARSSON, I. K. PERNESTÅL and B. JONSSON, Report 29, Swedish University of Agricultural Sciences, 1994.
23. F. THUVANDER, M. SJÖDAHL and L. A. BERGLUND, *J. Mater. Sci.* **35** (2000).
24. F. THUVANDER and L. A. BERGLUND, *J. Mater. Sci.* **35** (2000).
25. T. ENGØY, K. J. MÅLØE, A. HANSEN and S. ROUX, *Phys. Rev. Lett.* **73** (1994) 834.
26. S. W. J. BOATRIGHT and G. G. GARRET, *J. Mater. Sci.* **18** (1983) 2181.
27. M.-Y. HE and J. W. HUTCHINSON, *Int. J. Solids Structures* **25** (1989) 1053.

Received 27 July 1998
and accepted 12 May 2000